Density functional theory study of the reaction paths of reactions of $CH_3C(O)O_2$ radicals with HO_2 in the gas phase*

ZHOU Yuzhi[1,2], ZHANG Shaowen[1] and LI Qianshu[1]**

(1. State Key Laboratory of Explosion Science and Technology, Beijing Institute of Technology, Beijing 100081, China;
2. Beijing Institute of Education, Beijing 100044, China)

Received February 6, 2006; revised February 16, 2006

Abstract A DFT study on the reactions between $CH_3C(O)O_2$ and HO_2 radicals has been carried out. It is suggested that both the triplet and singlet potential surfaces involve a complex mechanism with the formation of loosely bound intermediate complexes of reactants and products. The reaction prefers to occur on the triplet surface to produce peracetic acid ($CH_3C(O)O_2H$) and triplet O_2 molecule. The $CH_3C(O)O_2H$ can further convert into $CH_3C(O)O$ and HO radicals.

Keywords: acetyl peroxy radicals, HO_2 radicals, reaction mechanism, DFT.

Acetyl peroxy radicals play a major role in the atmospheric degradation of organic compounds. In polluted atmospheres, the reaction between $CH_3C(O)O_2$ radical and NO_2 forms the well-known PAN (peroxyacetyl nitrate, $CH_3C(O)OONO_2$), an important organic contributor to photochemical smog. In less polluted atmospheres, the reactions between $CH_3C(O)O_2$ and HO_2 radicals become critical as NO_x levels may be low[1,2]. Niki et al. were the first to examine the reactions of $CH_3C(O)O_2$ with HO_2 radicals in a FTIR study of the photolysis of Cl_2 in the presence of CH_3CHO, HCHO and O_2[3]. According to analysis of products they showed that the reactions proceed via two channels:

$$CH_3C(O)O_2 + HO_2 \longrightarrow CH_3C(O)O_2H + O_2 \quad (1a)$$

$$CH_3C(O)O_2 + HO_2 \longrightarrow CH_3C(O)OH + O_3 \quad (1b)$$

with the branching ratio of 0.75 and 0.25 for channel (1a) and channel (1b), respectively, at 700 torr and 298 K. The subsequent kinetic studies[4,5] supported the results of Niki et al. However, Crawford et al.[6] obtained a branching ratio value of about 0.9∶0.1 using a similar technique with that of Niki et al. Moreover, Hasson et al.[7] reported another reaction channel: $CH_3C(O)O_2 + HO_2 \longrightarrow CH_3C(O)O + O_2 + OH$ (1c), giving the ratios of channel (1a): channel (1b): channel (1c) of about 0.4∶0.2∶0.4. The controversy in literatures requires further study on the title reactions. Our primary aim in this work is to identify the key intermediates and the reaction pathways and thereby to gain insight into the reaction mechanism.

1 Methodology

Considering the size of molecules involved in this study, we employed B3LYP method with the 6-31+G(d, p) and 6-311++G(d, p) basis sets to determine the geometries of the reactants, products, intermediates, and transition states. Each minimum we report has all real frequencies, and each transition structure has one imaginary frequency. The particular nature of a transition state has been determined by analyzing the motion described by the eigenvector associated to the imaginary frequency. Furthermore, the transition state was found to connect the proper reactants and products by the intrinsic reaction coordinate (IRC) method. The calculations were executed using the Gaussian 03 program[8].

2 Results and discussion

2.1 $CH_3C(O)O_2$ and HO_2 radicals

Fig. 1 shows the optimized geometries of reactants ($CH_3C(O)O_2$ and HO_2 radicals) at both B3LYP/6-31+G(d, p) and B3LYP/6-311++G(d, p) levels of theory. Our calculation shows that acetyl

* Supported by the National Natural Science Foundation of China (Grant No. 20373007)
** To whom correspondence should be addressed. E-mail: qsli@bit.edu.cn

peroxy radical has two (*E* and *Z*) possible conformations (*Z* or *E* with respect to the carbonyl group). The calculated relative energies between the *E*- and *Z*-conformation of $CH_3C(O)O_2$ radical are listed in Table 1. It can be seen that the energies of both conformations are close with the *E*-conformation being slightly more stable than the *Z*-conformation at both B3LYP/6-31+G(d, p) and B3LYP/6-311++G(d, p) levels of theory with the zero-point-energy (ZPE) correction. Besides, the calculation indicated that both conformations of $CH_3C(O)O_2$ radical have planar heavy atom framework.

Table 1. Relative energies of conformers of $CH_3C(O)O_2$ (kJ/mol)

$CH_3C(O)O_2$	B3LYP/6-31+G(d, p)		B3LYP/6-311++G(d, p)	
	E_{rel} (with ZPE)	E_{rel} (without ZPE)	E_{rel} (with ZPE)	E_{rel} (without ZPE)
Z-$CH_3C(O)O_2$	2.50	3.26	1.10	1.72
E-$CH_3C(O)O_2$	0.00	0.00	0.00	0.00

2.2 Reaction mechanism

The reactions between two open shell species, $CH_3C(O)O_2$ and HO_2 radicals, take place as they are approaching each other to interact on an attractive potential surface. And the spin state of the overall system they form can be either a singlet spin state or triplet. A picture of the optimized geometries and the calculated geometric parameters of various stationary points on both triplet and singlet surfaces is displayed in Fig. 1, and the corresponding lowest frequencies and zero-point energies (ZPE) are listed in Table 2. In general, the B3LYP/6-31+G(d, p) structures are consistent with the results from the B3LYP/6-311++G(d, p) calculations. Therefore we will just discuss the B3LYP/6-31+G(d, p) results later. The overall energetic profile based on the B3LYP/6-31+G(d, p) energies for the title reactions is shown in Fig. 2.

Table 2. The calculated vibrational frequencies (cm^{-1}) and the zero-point energies (kJ/mol) for stationary points involved in the title reaction at B3LYP/6-31+G(d, p) and B3LYP/6-311++G(d, p) level of theory

Stationary points	B3LYP/6-31+G(d, p)		B3LYP/6-311++G(d, p)	
	Lowest frequency	ZPE	Lowest frequency	ZPE
Z-$CH_3C(O)O_2$	68	136.39	68	135.89
E-$CH_3C(O)O_2$	136	137.16	136	136.51
HO_2	1166	37.03	1155	36.95
RM1	31	180.16	30	179.39
TS1	19i	178.67	16i	178.03
RM2	15	178.89	16	178.32

To be continued

Continued

Stationary points	B3LYP/6-31+G(d, p)		B3LYP/6-311++G(d, p)	
	Lowest frequency	ZPE	Lowest frequency	ZPE
TS2	274i	173.06	281i	172.18
PM1	16	180.95	18	180.55
$CH_3C(O)O_2H$	61	170.24	57	169.74
RM3	14	178.89	16	178.34
TS3	695i	168.44	763i	167.43
PM2	30	181.75	29	181.17
TS4	267i	181.68	273i	181.46
RM4	54	185.63	58	185.07
TS5	528i	174.25	719i	172.83
$CH_3C(O)OH$	71	161.98	73	161.54
O_3	698	16.84	710	16.62
TS6	183i	173.87	194i	172.84
PM3	22	175.15	19	174.12
$CH_3C(O)O$	38	125.10	40	124.61
HOOO	220	46.13	173	45.42
O_2	1641	9.82	1633	9.77

2.2.1 The triplet surface RM1 is a planar seven-membered-ring precursor or reactant complex. It has been found that the distance of H^1-O^2 and C^6-O^7 of RM1 increase about 0.001 nm compared to those of the isolated peroxy radicals ($CH_3C(O)O_2$ and HO_2). Meanwhile, C^6-O^5 distances show a decrease of 0.002 nm. The contact distances of $H^1 \cdots O^7$ and $H^9 \cdots O^3$ are 0.1818 nm and 0.2469 nm, respectively, which means there is strong hydrogen bond in RM1. RM1 can transform into another complex RM2 via a torsion transition state TS1. RM2 is a hydrogen-bonding complex also. The contact distances of $H^1 \cdots O^7$ of RM2 is 0.1934 nm, which means there is a moderately strong hydrogen bond between H^1 and O^7. TS2 is a triplet transition state which describes the H-abstraction process on the triplet surface. The $O^2H^1O^4$ angle in TS2 is 163°. Compared to RM2, the breaking $H^1 \cdots O^2$ bond of TS2 is only elongated by 0.0040 nm, and the forming $O^2 \cdots O^3$ bond is 0.1557 nm. Therefore TS2 is a reactant-like transition state. PM1 is a triplet product complex. The contact distance of $H^1 \cdots O^3$ of PM1 is 0.2556 nm, which means a weak hydrogen bond between H^1 and O^3. The dihedral angle of $O^2O^3O^4O^5$ in PM1 is 0.0°, which indicates that the $O^2=O^3$ moiety in PM1 locates exactly in the peracetic acid moiety plane. The molecular orbital of PM1 shows that the two molecular orbital corresponding to the two π^* orbital of the dioxygen moiety ($O^2=O^3$) are singly occupied and have the same spin state. In keeping with these descriptions, the spin densities on O^2 and O^3 in PM1 are 0.99 and 1.01, respectively. In a word, PM1 is formed by peracetic acid ($CH_3C(O)O_2H$) and triplet O_2 molecule.

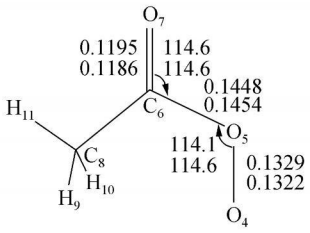

E-$CH_3C(O)O_2$

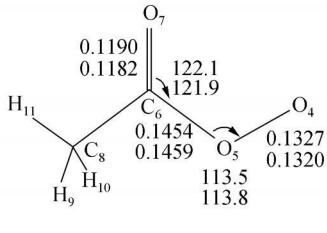

Z-$CH_3C(O)O_2$

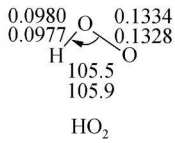

HO_2

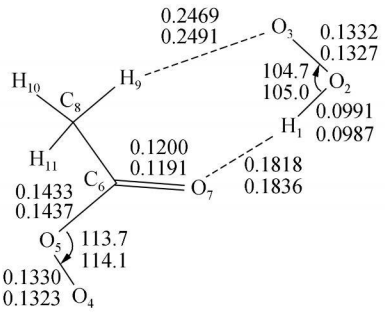

RM1

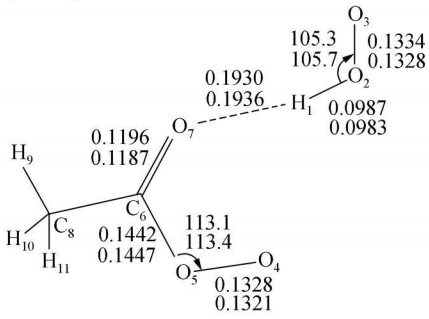

TS1

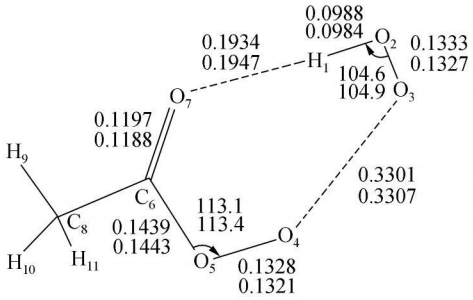

RM2

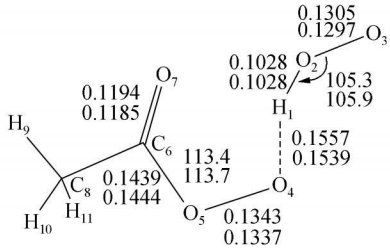

TS2

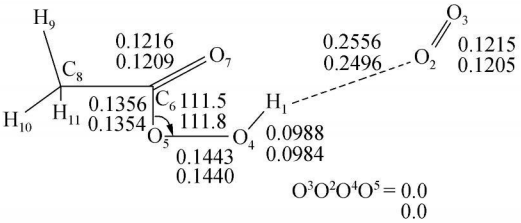

PM1

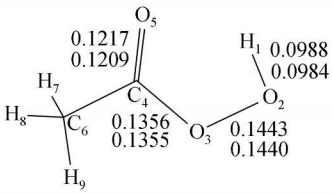

$CH_3C(O)O_2H$

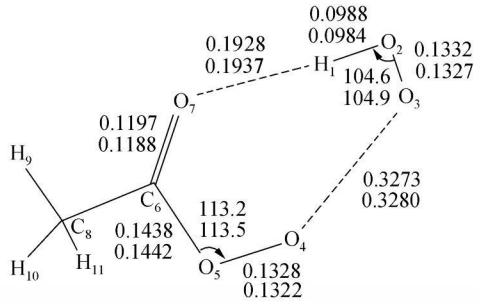

RM3

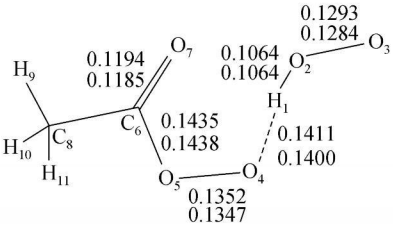

TS3

(To be continued)

(Continued)

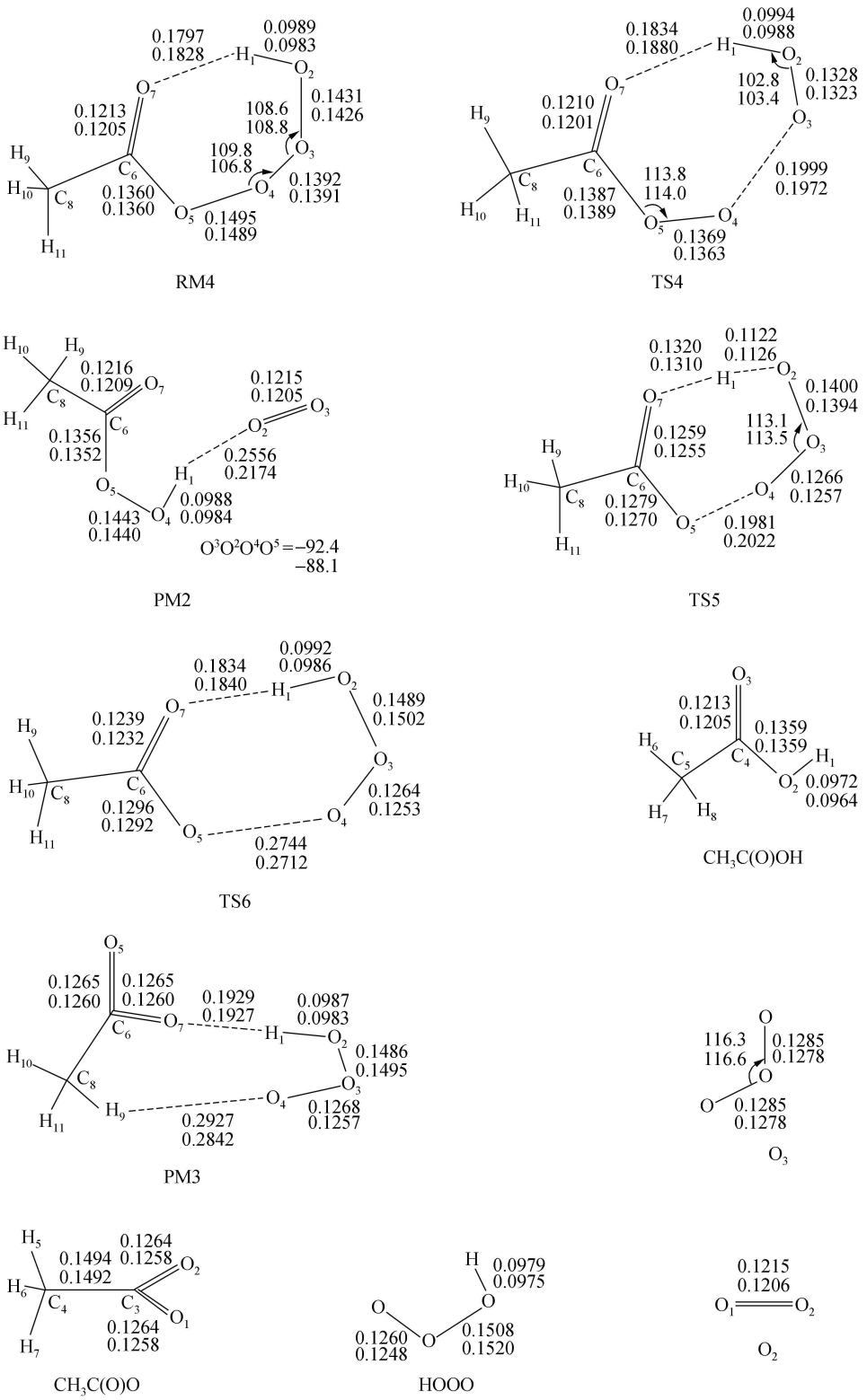

Fig. 1. Optimized geometries of stationary points at the B3LYP/6-31+G(d, p) and B3LYP/6-311++G(d, p) level of theory. For the structures with two entries, the upper data are obtained at the B3LYP/6-31+G(d, p) level and the lower data are obtained at the B3LYP/6-311++G(d, p) level, respectively. The bond distances are in nm, and the angles are in degree.

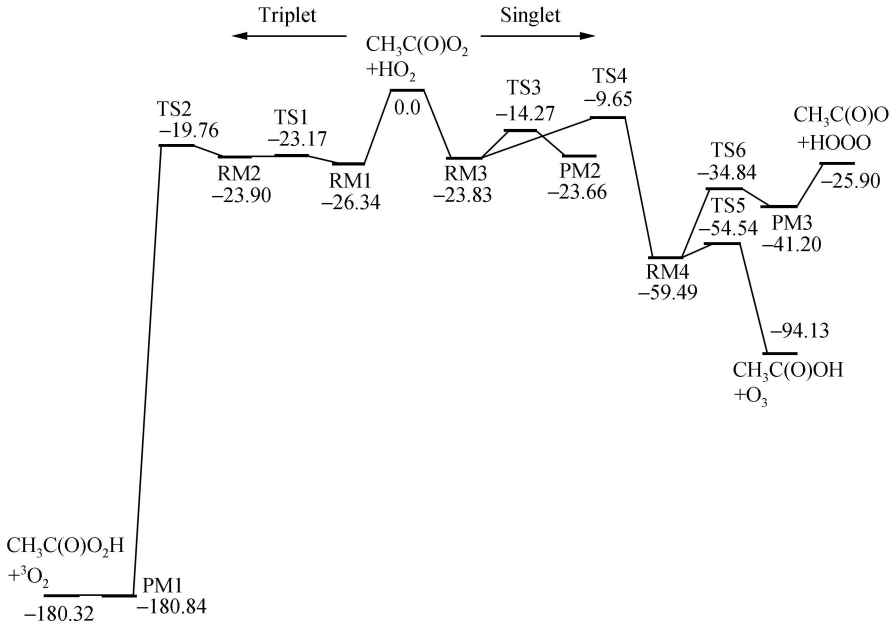

Fig. 2. The overall profile of the potential surface for the reaction of $CH_3C(O)O_2$ with HO_2 calculated at B3LYP/6-31+G(d, p) levels with ZPE correction (kJ/mol).

The reaction $CH_3C(O)O_2+HO_2 \longrightarrow CH_3C(O)O_2H+O_2$ is highly exothermic. The calculated reaction heat is 182 kJ/mol which is in agreement with the literature value of 180 kJ/mol[9]. It is noting that $CH_3C(O)OH$ can decompose to $CH_3C(O)O$ and HO radicals via simple O-O bond scission. This process needs energy of 153 kJ/mol at B3LYP/6-31+G(d, p) level of theory. Therefore it is reasonable that a fraction of nascent $CH_3C(O)O_2H$ can further convert into $CH_3C(O)O$ and HO radicals and thus affect the product distribution in the $CH_3C(O)O_2+HO_2$ reactions.

2.2.2 The singlet surface As can be seen from Fig. 2, there are three product channels on the singlet surface. The initial reactant complex is RM3 which has nearly the same geometries and energy as those of RM2. Furthermore, RM3 has surprisingly similar electron density distributions as those of RM2. For example, the spin densities on O^3 and O^4 are 0.72 and 0.77 respectively, in the triplet reactant complex RM2 and −0.71 and 0.78 in the singlet reactant complex RM3. The similarity between RM2 and RM3 may be attributed to the loose structure of these reactant complexes as the contact distance of $O^3...O^4$ is 0.33 nm in RM2 as well as in RM3. Starting from RM3, there are two possible reactions pathways. One is the hydrogen abstraction which leads to the product complex PM2 via transition state TS3. The other is the conversion of RM3 to a much deeper well RM4 via transition state TS4. Similar to TS2, the singlet hydrogen abstraction transition state TS3 is a reactant-like transition state either. The breaking H...O bond is only slightly stretched to 0.1064 nm and the forming H...O bond is 0.1411 nm. For PM2, only one oxygen atom of the dioxygen moiety ($O^2=O^3$) locates in the peracetic acid moiety plane and the dioxygen moiety ($O^2=O^3$) is nearly perpendicular to the peracetic acid moiety plane ($O^2O^3O^4O^5=97.5^\circ$). The molecular orbitals of PM2 show that two paired electrons occupy one of the molecular orbitals which corresponds to the two Π^* orbitals of the dioxygen moiety ($O^2=O^3$) leaving the other Π^* orbitals empty. Moreover, the spin densities on O^2 and O^3 are 0.00 in PM2. Therefore PM2 is a complex of peracetic acid ($CH_3C(O)O_2H$) and singlet O_2 molecule. RM4 is a tetroxide intermediate and has many conformations due to the torsions of O_4 skeleton. For simple purpose, only the most stable conformer is shown in Fig. 1. It is shown that the central O-O distance (O^3-O^4) in RM4 appears to be 0.004 nm −0.010 nm smaller than other O-O distances. The dihedral angle $O^2O^3O^4O^5$ is 106°. The distance between H^1 and O^7 is about 0.18 nm which means there is a strong hydrogen bond between H^1 and O^7 in RM4. With respect to the initial reactants ($CH_3C(O)O_2+HO_2$), the potential well depth of

RM4 is 59.5 kJ/mol, deeper than that of RM3 by 35.7 kJ/mol. Once RM4 is formed, it can easily undergo an inner hydrogen transfer to emit O_3 via the seven-membered-ring transition state TS5. TS5 is a concerted transition state with a barrier height of 4.9 kJ/mol. The distances of $H^1...O^2$ and $O^4...O^5$ of TS5 are 0.1122 nm and 0.1981 nm, respectively. Decomposition of RM4 may also occur via O-O bond scission to give $CH_3C(O)O$ and HOOO radicals. This process involves a transition state TS6. TS6 is a product-like transition state and its barrier height is 24.6 kJ/mol, which is 19.7 kJ/mol higher than that of TS5. Thus it is not a preferable reaction path. However, the energy of TS6 is 34.8 kJ/mol lower than the total energy of the initial reactants. It is possible that a fraction of $CH_3C(O)O$ and HOOO could be produced. PM3 is a complex formed by $CH_3C(O)O$ and HOOO. Like other complexes, there is a hydrogen bond in PM3. The contact distance of $H^1...O^7$ of PM3 is 0.1929 nm and the $CH_3C(O)O$ moiety plane is nearly perpendicular to HOOO moiety plane ($O^3O^7C^6O^5 = 99.7^\circ$). An equilibrium $HO + O_2 \rightleftharpoons HOOO$ may exist at room temperature[10], thus the finial products would be $CH_3C(O)O + HO + O_2$.

3 Summary

In this paper, the reactions between $CH_3C(O)O_2$ and HO_2 radicals have been studied by DFT calculations. It is suggested that both the triplet and singlet potential surfaces involve a complex mechanism with the formation of loosely bound intermediate complexes of reactants and products. The hydrogen abstraction on the triplet surface possesses the lowest barrier and the biggest value of reaction heat, thus the reaction prefers to occur on the triplet surface. The products on the triplet surface are peracetic acid ($CH_3C(O)O_2H$) and triplet O_2 molecule. Peracetic acid may further decompose to $CH_3C(O)O + HO$ radicals. There is a very deep well on the singlet surface. Ozone can be formed via a seven-membered-ring concerted transition state. Singlet O_2 molecule, peracetic acid, as well as $CH_3C(O)O + HO$ radicals can also be produced on the singlet surface. The energies of all the involved transition states are lower than the total energy of the reactants, which implies that all the reactions may process fast. It should be emphasized that the present calculation is only of semi-quantity. Further elaborate investigations of the mechanism and dynamic characteristics of the title reactions are clearly required.

References

1 Wallington T. J., Dagaut, P., Kurylo, M. J. Ultraviolet absorption cross sections and reaction kinetics and mechanisms for peroxy radicals in the gas phase. Chem. Rev., 1992, 92: 667—710.

2 Tyndall G. S., Cox R. A., Granier C. et al. Atmospheric chemistry of small peroxy radicals. J. Geophys. Res., D2001, 106: 12157—12182.

3 Niki H., Maker P. D., Savage C. M. et al. FTIR study of the kinetics and mechanism for Cl-atom-initiated reactions of acetaldehyde. J. Phys. Chem., 1985, 89: 588—591.

4 Moortgat G. K., Veyret B., Lesclaux R. Kinetics of the reaction of HO_2 with $CH_3C(O)O_2$ in the temperature range 253—368 K. Chem. Phys. Lett., 1989, 160: 443—447.

5 Tomas A., Villenave E., Lesclaux R. Reactions of the HO_2 radicals with CH_3CHO and $CH_3C(O)O_2$ in the gas phase. J. Phys. Chem. A, 2001, 105: 3505—3514.

6 Crawford M. A., Wallington T. J., Szente J. J. et al. Kinetics and mechanism of the acetylperoxy + HO_2 reaction. J. Phys. Chem. A, 1999, 103: 365—378.

7 Hasson A. S., Tyndall G. S., Orlando J. J. A product yield study of the reaction of HO_2 radicals with ethyl peroxy ($C_2H_5O_2$), acetyl peroxy ($CH_3C(O)O_2$), and acetonyl peroxy ($CH_3C(O)CH_2O_2$) radicals. Phys. Chem. A, 2004, 108: 5979—5989.

8 Frisch M. J., Trucks G. W., Schlegel H. B. et al. Gaussian 03, revision B. 05; Gaussian Inc.: Pittburgh, PA, 2003.

9 IUPAC subcommittee on gas kinetic data evaluation-data sheet HOx-VOC54. http://www.iupac.kinetic.ch.cam.ac.uk/. [2002-8-9]

10 Jungkamp T. P. W. and Seinfeld J. H. The enthalpy of formation of trioxy radicals ROOO. Chem. Phys. Lett., 1996, 257: 15—22.